7.4 AN ELECTRON ENERGY LOSS SPECTROSCOPY STUDY OF HELIUM BUBBLES IN NANOSTRUCTURED FERRITIC ALLOYS

— Y. Wu, R. G. Odette, T. Yamamoto, (University of California, Santa Barbara); J. Ciston, (Lawrence Berkeley National Laboratory); and P. Hosemann (University of California, Berkeley)

OBJECTIVE

Understanding and predicting the fate of helium that is generated in large quantities within fusion irradiation environments requires experiments and modeling methods to understand the partitioning between various bubble sites.

SUMMARY

Here we compare a measurement of the helium content in bubbles with a model based on the capillary approximation and a high-pressure equation of state. Electron Energy-Loss Spectroscopy (EELS) measurements on bubbles were carried out using the TEAM 0.5 microscope at the National Center for Electron Microscopy and Lawrence Berkeley Laboratory (LBL). The EELS energy shift can be related to the helium atom density. The best estimate of the helium density was ≈ 61±2.8 He atoms/nm^3 for bubbles with radii of ≈ 1.36±0.3 nm. These results are reasonably consistent with a high pressure EOS assuming a simple capillary model and surface energy of 1.8 J/m^2.

PROGRESS AND STATUS

Introduction

Nanostructured ferritic alloys (NFA) manage helium by trapping it in small bubbles at the interfaces between nano-scale oxide features and the Fe-Cr matrix [1,2]. Thus it is important to know the relation between the bubble size and helium content. Assuming the simple capillary approximation, the gas pressure, p, balances the surface tension as p = 2g/r, where g is the surface energy and r is the bubble radius (or radius of curvature). Hence, *very small* high-pressure bubbles can efficiently store helium in a way that prevents its deleterious effects like void nucleation and other manifestations of radiation damage. The pressure, p, is related to the helium atom density, r (here in units of the number of atoms/nm^3), by a high-pressure equation of state (EOS). The corresponding number of helium atoms (m_{He}) in a bubble also depends on its morphology and the effects of finite bubble size.

Electron Energy-Loss Spectroscopy (EELS) was carried out using small probe transmission electron microscopy methods (TEM) that can be used to measure the helium density in bubbles [3-5]. There is a blue energy shift for the 1s-2p transition of helium, ΔE, which is related to atom density in the bubbles. Fréchard et al., reported the relationship between r and the blue shift as, $\Delta E = 0.019\ r + 1.36$; they also found that all the results in the literature can be fitted by $\Delta E = 0.036\ r + 0.39$. Similar relations and theoretical models of the blue energy shift and r are given in [4,5].

The helium bubbles in irradiated NFA are small (typical diameters, d < 3 nm) and have a narrow size distribution. The bubble size probed here is about 33% smaller than the smallest previously reported [3].

Experimental Procedure

Dual ion irradiations in the DuET facility at Kyushu University created a population of helium bubbles in NFA MA957 and a developmental 14YWT heat called PM2. Table 1 lists the alloy compositions. Both NFA MA957 and PM2 were irradiated at 650°C. The actual dpa, He and He/dpa vary with ion beam penetration depth into the sample. The areas examined in both alloys were at a depth of ≈ 1.3 μm from the surface, corresponding to 118 dpa at a rate of 2.8×10^{-3} dpa/s and 2750 appm He. Lift-out TEM specimens were prepared by using a FEI Helios focused ion beam microscope (FIB). A final lift out cleaning step used a low energy 2 KV, 5.5 pA beams to minimize gallium ion damage. Electron Energy-Loss Spectroscopy (EELS) was carried out on the bubbles using the TEAM 0.5 double aberration corrected TEM at the National Electron Microscopy Center (NCEM) at LBL.

It is difficult to obtain He 1s-2p signals from the bubbles with radius < 2 nm. However, by using a combination of so-called "spectra image" (SPIM) mode and the "chronospim" approach [3,4], it was possible to increase the signal to noise ratio sufficiently to evaluate ΔE. The chronospim approach involves acquiring, realigning and summing a large number of spectra [3]. We acquired 50-100 spectra from different, but similarly sized (d < 3nm) bubbles in the two alloys. The helium 1s-2p peaks were established by Gaussian curve fits that subtracted a fitted plasmon signal from the total EELS spectrum. High angle annular dark field (HAADF), which is superior to bright field through focus imaging for detecting voids, was used to measure the sizes of the bubbles probed.

Table 1. Alloy composition (in wt.%)

Alloy	Cr	Ti	W	Mo	Y	Fe
MA 957	14.0	0.9		0.3	0.25	84.55
PM2	14.0	0.35	3.0		0.30	82.35

Results and Discussion

Figure 1 shows that the helium bubbles are small and quite uniform in size, lying in the range of d ≈ 2-3 nm. Table 2 compares the bubble size range characterized here to those in previous studies.

As noted above it is difficult to measure the He 1s-2p peak for an individual EELS spectrum, because it overlaps the plasmon peak of the matrix. However, it is possible to realign and sum many peaks as shown in Figure 2 (e.g., the chronospim approach). Figure 2a shows a realigned and summed EELS spectrum with the matrix plasmon signal fitted by a Gaussian curve (red line). Figure 2b shows the helium 1s-2p signals obtained by subtracting the plasmon curve from the total realigned and summed EELS spectrum. The helium signal is also fitted using a Gaussian curve to establish the peak energy. Note the different appearance of the curve in Figure 2a is due to the large number of counts acquired in this case.

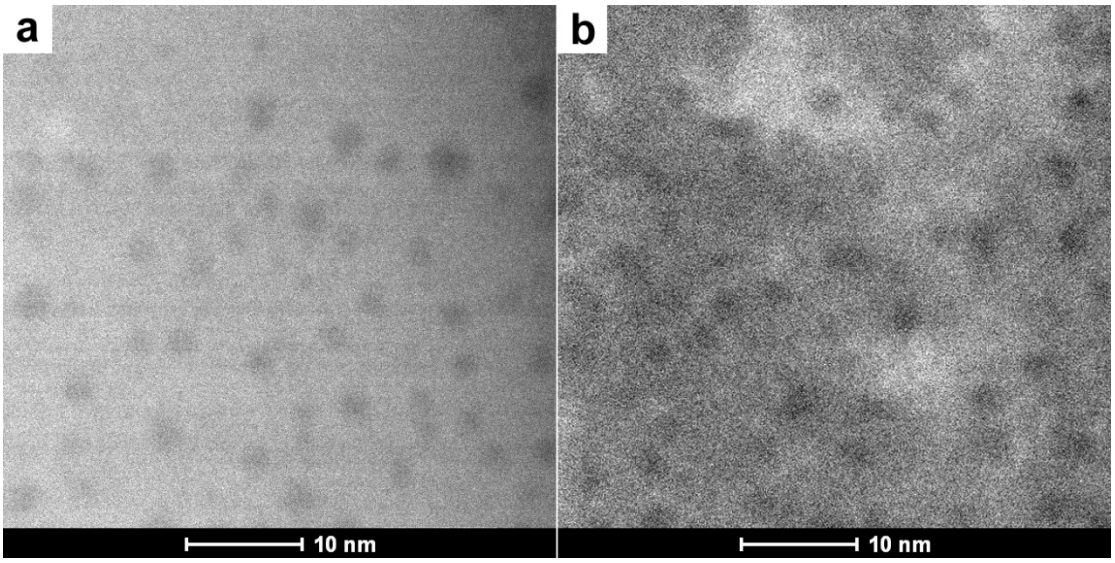

Figure 1. HAADF images of helium bubbles in: a) PM2; and, b) MA957.

Table 2. Comparison of bubble size in the literature measuring He density-using EELS.

	Bubble diameter (nm)
S. Frechard, et al., (Ref. 1)	4-12
D. Taverna, et al., (Ref. 2)	5-24
J. C. Rife, et al., (Ref. 3)	~ 5
This report	< 3

The energy 1s-2p peak energy for a free helium atom is 21.2 eV. The measured E ≈ 23.7 eV was found for the helium in bubbles in MA957, so ΔE = 2.5 eV. The average radius of the bubbles from which EELS spectra was <r> ≈ 1.34 nm, with r ranging from 1.01 to 1.68 nm. Using the relationship between the energy shift (ΔE) and the helium density ρ as $\Delta E \approx 0.036\rho + 0.39$, yields $\rho = 58.6/nm^3$. Using $\Delta E = 0.019\,\rho + 1.36$, yields $\rho \approx 60.0/nm^3$. The corresponding ΔE for the bubbles in PM2 was 2.6 eV, yielding corresponding $\rho \approx 61.4$ and $65.3/nm^3$, respectively. The average radius of the bubbles in PM2 was <r> ≈ 1.37 nm, with r ranging from 1.15 to 1.65 nm. The uncertainty of ΔE is estimated to be less than ≈ ±0.2 eV, corresponding to an average maximum variation of ρ of ≈ ± 11. The different ρ–ΔE correlations suggest a smaller degree of helium density variability, and the overall average and standard deviation of ρ are $61.3 \pm 2.8/nm^3$. The average radius of the bubbles from which EELS spectra were obtained was <r> ≈ 1.36±0.3 nm. This corresponds to a He/vacancy ratio of ≈ 0.72.

Figure 4 shows the ρ reported in the literature (filled red circles) [3], along the current results, plotted as a function of 1/r. The Fréchard et al. data is for a 9Cr tempered martensitic steel that was implanted with 5000 appm helium at 550°C. The pseudo error bars show the estimated ranges of ρ and 1/r for the bubbles examined in this study. The solid and dashed lines are predictions based on a simple high pressure EOS [6], assuming $p = 2\gamma/r$, using for $\gamma = 1.8\ J/m^2$ for 650 (current study) and 550°C (Fréchard), respectively. The agreement is good for the

current results, but only in more qualitative agreement with the previous measurements on somewhat larger helium bubbles. In this case the capillary EOS model over-predicts and under-predicts the ρ at larger bubble and smaller bubble sizes, respectively. That is the slope of the ρ versus 1/r data trend is higher than predicted. In the size range of about $r \approx 2.1 \pm 0.2$ nm, the measured ρ average ≈ 28% higher than the prediction. Extrapolating the model suggests that the He/vacancy ratio approaches 1 at $r < 0.5$ nm.

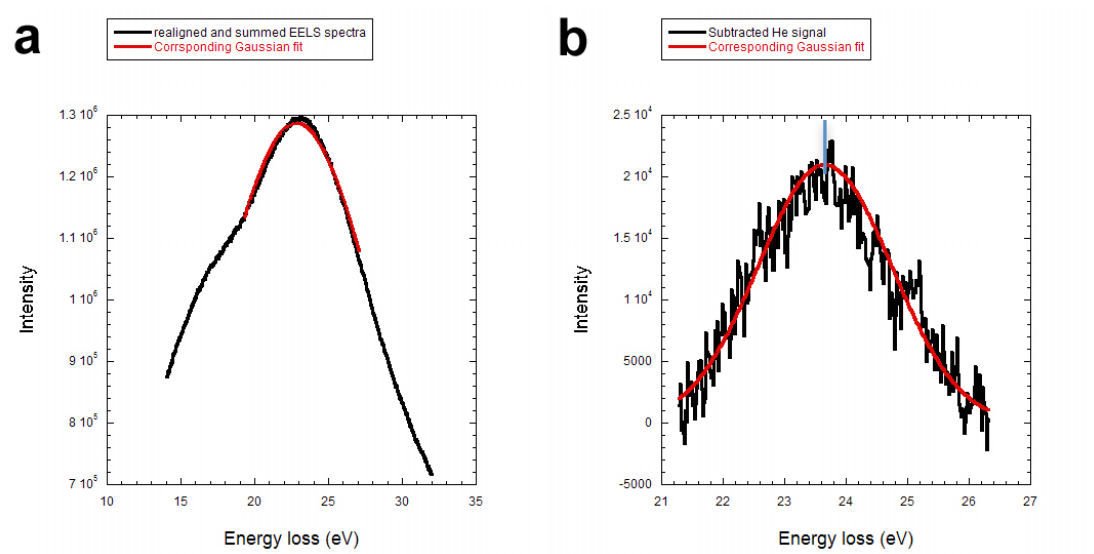

Figure 2. Gaussian fit curves (red) to MA957 EELS spectra data: a) the realigned and summed spectra from many bubbles with similar size and the fit to the plasmon peak; and b) the fitted subtracted helium signal.

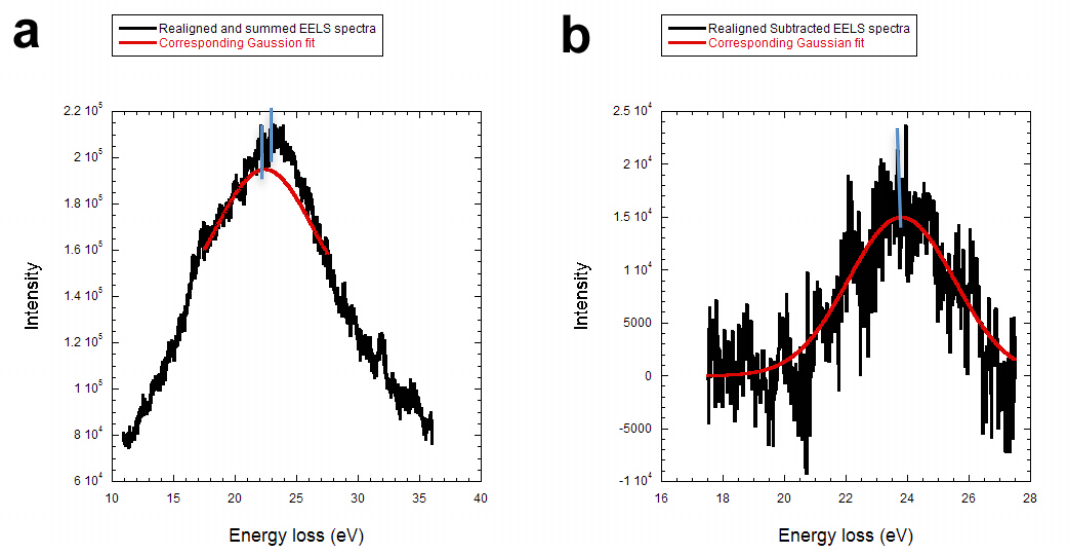

Figure 3. Gaussian fit curves (red) to PM2 EELS spectra data: a) the realigned and summed EELS spectra from many bubbles with similar size and the fit to the plasmon peak; and b) the subtracted helium signal.

More quantitatively, the model predicts ρ = 57.9 He/nm^3 for r = 1.36 nm at 650°C compared to the measured average of 61.3 He/nm^3. The effect of temperature is modest, with the predicted values of ρ varying from 65.7 He/nm^3 at 300°C to 55.2 He/nm^3 at 800°C. Variations in γ from 1.6 to 2 J/m^2 result in predicted ρ of 55.1 to 60.4 He/nm^3, respectively.

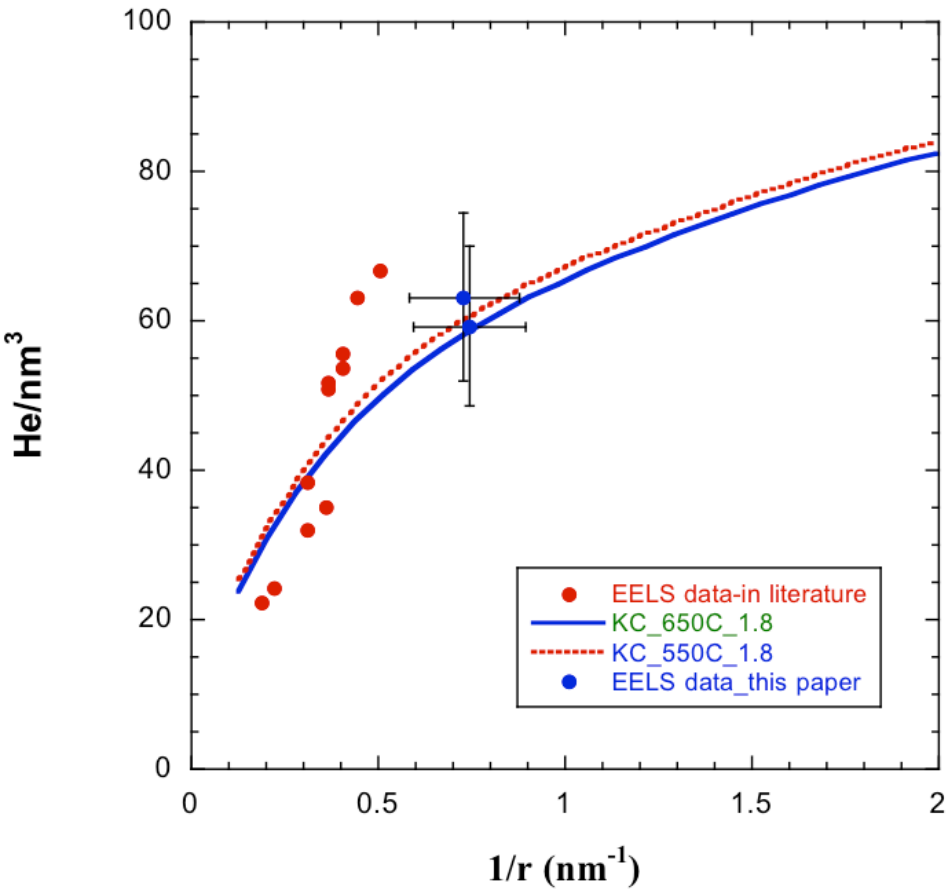

Figure 4. Predicted versus measured helium atom densities as a function of the inverse bubble radius.

DISCUSSION AND FUTURE WORK

The results in this study extend EELS measurements of helium density in bubbles at 650°C down to an average radius of r ≈ 1.36±0.3 nm of r ≈ 61.3±2.8 He/nm^3 are in good agreement with a simple model. The measured r corresponds to helium to vacancy ratio, He/V≈ 0.72 for relative small bubble size. The model under-predicts previously reported r data by about 28% for larger r = 2±0.2 nm bubbles formed during helium implantation at 550°C. In the temperature range from 550 to 650°C, the predicted He/vacancy ratio approaches 1 at r ≈ 0.5 nm and drops to ≈ 0.24 at r = 10 nm.

Through focus series TEM measurements of the helium bubble average size and number density in the implanted regions in this study yielded 2.3 nm and 5.9x10^{23}/m^3, respectively. Based on the EELS measurements of ρ, this corresponds to a total amount of helium in spherical bubbles of 2605 appm, in good agreement with the estimate of implanted helium of 2750 appm.

Future work will evaluate other nominally more rigorous equations of state after both Stoller [7] and Caro [8] and co-workers. The objective of quantifying helium partitioning and balances will also be pursued. This will require evaluation of the morphology of bubbles on precipitates and more careful consideration of various sources of experimental and modeling uncertainties.

ACKNOWLEDGEMENT

Electron Microscopy experiments were performed at the National Center for Electron Microscopy, Lawrence Berkeley National Laboratory, which is supported by the DOE BES under Contract # DE-AC02-05CH11231.

REFERENCES

[1] G. R. Odette, M. J. Alinger, and B. D. Wirth, *Annu. Rev. Mater. Res.* **38** (2008) 471.
[2] G. R. Odette and D. T. Hoelzer, *JOM* **62** (2010) 84.
[3] S. Fréchard, M. Walls, M. Kociak, J.P. Chevalier, J. Henry, and D. Gorse, *J. Nucl. Mater.* **393** (2009) 102.
[4] D. Taverna, M. Kociak, O. Stephan, A. Fabre, E. Finot, B. Decamps, and C. Colliex, *Phys. Rev. Lett.* **100** (2008) 035301.
[5] J. C. Rife, S. E. Donnelly, A. A. Lucas, J. M. Gilles, and J. J. Ritsko, *Phys. Rev. Lett.* **46** (1981) 1220.
[6] R. E. Stoller and G. R. Odette, *J. Nucl. Mater.* **131** (1985) 118.
[7] R. E. Stoller and Y. N. Osetskiy, Fusion Reactor Materials Program, Dec. 31, 2012, DOE/ER-0313/53 (2012) 100.
[8] A. Caro, J. Hetherly, A. Stukowski, M. Caro, E. Martinez, S. Srivilliputhur, L. Zepeda-Ruiz, and M. Nastasi, *J. Nucl. Mater.* **418** (2011) 261.